



COVID-19 Research Tools

Defeat the SARS-CoV-2 Variants

InvivoGen



Hepatitis B Virus and DNA Stimulation Trigger a Rapid Innate Immune Response through NF- κ B

This information is current as of February 26, 2022.

Masato Yoneda, Jinhee Hyun, Silvia Jakubski, Satoru Saito, Atsushi Nakajima, Eugene R. Schiff and Emmanuel Thomas

J Immunol 2016; 197:630-643; Prepublished online 10 June 2016;

doi: 10.4049/jimmunol.1502677

<http://www.jimmunol.org/content/197/2/630>

Supplementary Material <http://www.jimmunol.org/content/suppl/2016/06/10/jimmunol.1502677.DCSupplemental>

References This article **cites 36 articles**, 12 of which you can access for free at: <http://www.jimmunol.org/content/197/2/630.full#ref-list-1>

Why *The JI*? Submit online.

- **Rapid Reviews! 30 days*** from submission to initial decision
- **No Triage!** Every submission reviewed by practicing scientists
- **Fast Publication!** 4 weeks from acceptance to publication

**average*

Subscription Information about subscribing to *The Journal of Immunology* is online at: <http://jimmunol.org/subscription>

Permissions Submit copyright permission requests at: <http://www.aai.org/About/Publications/JI/copyright.html>

Email Alerts Receive free email-alerts when new articles cite this article. Sign up at: <http://jimmunol.org/alerts>



Hepatitis B Virus and DNA Stimulation Trigger a Rapid Innate Immune Response through NF- κ B

Masato Yoneda,^{*,†} Jinhee Hyun,[‡] Silvia Jakubski,[‡] Satoru Saito,[§] Atsushi Nakajima,[§] Eugene R. Schiff,^{*,†} and Emmanuel Thomas^{*,†}

Cell-intrinsic innate immunity provides a rapid first line of defense to thwart invading viral pathogens through the production of antiviral and inflammatory genes. However, the presence of many of these signaling pathways in the liver and their role in hepatitis B virus (HBV) pathogenesis is unknown. Recent identification of intracellular DNA-sensing pathways and involvement in numerous diverse disease processes including viral pathogenesis and carcinogenesis suggest a role for these processes in HBV infection. To characterize HBV-intrinsic innate immune responses and the role of DNA- and RNA-sensing pathways in the liver, we used in vivo and in vitro models including analysis of gene expression in liver biopsies from HBV-infected patients. In addition, mRNA and protein expression were measured in HBV-stimulated and DNA-treated hepatoma cell lines and primary human hepatocytes. In this article, we report that HBV and foreign DNA stimulation results in innate immune responses characterized by the production of inflammatory chemokines in hepatocytes. Analysis of liver biopsies from HBV-infected patients supported a correlation among hepatic expression of specific chemokines. In addition, HBV elicits a much broader range of gene expression alterations. The induction of chemokines, including CXCL10, is mediated by melanoma differentiation-associated gene 5 and NF- κ B-dependent pathways after HBV stimulation. In conclusion, HBV-stimulated pathways predominantly activate an inflammatory response that would promote the development of hepatitis. Understanding the mechanism underlying these virus–host interactions may provide new strategies to trigger noncytotoxic clearance of covalently closed circular DNA to ultimately cure patients with HBV infection. *The Journal of Immunology*, 2016, 197: 630–643.

Cell-intrinsic innate immunity provides a first line of defense to thwart invading viral pathogens (1). Production of type I and III IFN are critical aspects of this initial response,

with type III/IFNL being a significant component of the antiviral response in the liver (2). Significant progress has been made recently relating to how cells recognize pathogen-derived RNA, although it has been less clear how cells in the liver trigger innate immune signaling in response to DNA species originating from microbes.

Hepatitis B virus (HBV) has a DNA genome that is converted to RNA intermediates through the activity of cellular RNA polymerases (3–5). HBV-associated liver damage is thought to be the consequence of a long-lasting cytolytic immune response against infected hepatocytes (6). Using experimentally infected chimpanzees, microarray analyses suggested that HBV, early in infection, does not modulate host cellular gene transcription significantly and would induce neither innate antiviral responses in hepatocytes nor intrahepatic innate immune responses (7). After this study, HBV was designated as a “stealth virus” (8), but this may not be the case (9). Furthermore, a study demonstrated that HBV may be cleared from infected hepatocytes before any detectable adaptive immune response (10), thus suggesting that innate immunity or antiviral responses at the level of infected cells could play an important role. In addition, the source of chemokines that are detected in HBV infection such as CXCL10/IFN- γ inducible protein 10 has been an area of debate. Initial studies demonstrated that these chemokines were mainly produced after an adaptive immune response (11–13). However, more recent studies have shown that HBV can also stimulate production of chemokines such as CXCL10 at early time points (14–16). Unfortunately, antiviral innate immunity against HBV that occurs minutes after virus contact is an area that has been neglected and necessitates further investigation. In addition, as compared with RNA viruses such as hepatitis C virus (HCV), less is known about how human hepatocytes recognize DNA viruses such as HBV and their replicative RNA intermediates.

Recent breakthroughs in our understanding of DNA-dependent signaling processes arose through the discovery of proteins that

*Schiff Center for Liver Diseases, University of Miami Miller School of Medicine, Miami, FL 33136; [†]Sylvester Cancer Center, University of Miami Miller School of Medicine, Miami, FL 33136; [‡]Department of Cell Biology, University of Miami Miller School of Medicine, Miami, FL 33136; and [§]Department of Gastroenterology and Hepatology, Yokohama City University Graduate School of Medicine, Yokohama 226-0004, Japan

ORCID: 0000-0003-2823-1225 (J.H.); 0000-0002-5666-5218 (S.S.); 0000-0002-6263-1436 (A.N.); 0000-0002-0978-2040 (E.R.S.).

Received for publication December 30, 2015. Accepted for publication May 6, 2016.

This work was supported by the Miami Center for AIDS Research at the University of Miami Miller School of Medicine, supported by National Institutes of Health Grant P30AI073961 (to E.T.), and the Miami Clinical and Translational Science Institute KL2 program (to E.T.).

E.T. and M.Y. created study concept and design; M.Y., J.H., S.J., S.S., E.R.S., and A.N. performed acquisition of data; M.Y. and E.T. did analysis and interpretation of data; M.Y. and E.T. drafted the manuscript; M.Y. performed statistical analysis; and E.T. oversaw study supervision.

The microarray data presented in this article have been submitted to the Gene Expression Omnibus under accession number GSE69590.

Address correspondence and reprint requests to Dr. Emmanuel Thomas, Department of Cell Biology, University of Miami Miller School of Medicine, 1550 NW 10th Avenue, Papanicolaou Building, Room PAP 514, Miami, FL 33136. E-mail address: Ethomas1@med.miami.edu

The online version of this article contains supplemental material.

Abbreviations used in this article: ALT, alanine aminotransferase; cccDNA, covalently closed circular DNA; 2'3'-cGAMP, cyclic [G(2',5')pA(3',5')p]; cGAS, cyclic GMP-AMP synthase; GEq, genome equivalent; HBV, hepatitis B virus; HCV, hepatitis C virus; IKK γ , I κ B kinase γ ; IRF3, IFN regulatory factor 3; ISD, IFN stimulatory DNA; ISG, IFN-stimulated gene; MDA5, melanoma differentiation-associated gene 5; PHH, primary human hepatocyte; poly(dA:dT), poly(deoxyadenylic-deoxythymidylic); poly(dG:dC), poly(deoxyguanylic-deoxycytidylic) acid; poly(I:C), polyinosinic:polycytidylic acid; qPCR, quantitative PCR; RIG-I, retinoic acid-inducible gene; RMA, robust multiarray average; RSAD2, radical S-adenosyl methionine domain-containing protein 2; siRNA, small interfering RNA; STING, stimulator of IFN genes; TBK1, TANK-binding kinase 1.

Copyright © 2016 by The American Association of Immunologists, Inc. 0022-1767/16/\$30.00

have been implicated in the sensing of these nucleic acids (17). DNA has been shown to directly or indirectly through RNA intermediates induce cytokines through the activation of transcription factors including NF- κ B (18, 19). However, little is known about these DNA-sensing mechanisms, which can be tissue specific, in hepatocytes and their role in production of type III IFN/IFNL or HBV antiviral responses. To investigate the pathways involved in sensing of HBV DNA and associated RNA intermediates in human hepatocytes within minutes to hours after stimulation, we used several *in vitro* models including primary human hepatocytes (PHHs) and the HepaRG cell line that have functional intrinsic innate immune responses as opposed to transformed hepatoma cell lines (20, 21). Because HBV has a DNA genome that is transcribed into viral RNAs (3–5), characterization of DNA-sensing pathways and associated RNA intermediaries are needed to gain insight into the mechanisms by which HBV can rapidly induce an innate response in human hepatocytes.

Materials and Methods

Cells

HepaRG cells (Life Technologies) were maintained in William's medium E (Life Technologies) supplemented with additives for the HepaRG growth medium (Life Technologies) and with 50 U/ml penicillin/streptomycin (Invitrogen), GlutaMAX 2 mM (Life Technologies) and cultured at 37°C in humidified incubators at 5% CO₂ (22). To obtain differentiation of HepaRG, we maintained cells for 2 wk in standard medium and then for 2 wk in medium supplemented with 1.8% DMSO (cell culture grade; Sigma, St. Louis, MO) (23). HepG2/NTCP cells were maintained at 37°C in 5% CO₂ in DMEM (Life Technologies) containing 10% FBS with 50 U/ml penicillin/streptomycin. HepG2.2.15 cells (HBV serotype ayw, genotype D) were maintained at 37°C in 5% CO₂ in DMEM with 10% FBS and 400 μ g/ml G418 (Life Technologies) (24). PHHs and HepaRG cells were purchased from Thermo Fisher Scientific. The HepG2/NTCP cell line was provided by C. Seeger (Fox Chase Cancer Center, Philadelphia, PA).

HBV preparation and stimulation

HBV used in this study was derived from HepG2.2.15 cells. Media were cleared through a 0.45- μ m filter and precipitated with PEG-*it* Virus Precipitation Solution (System Biosciences) according to the manufacturer's instructions. The precipitates were resuspended in PBS containing 25% FBS at 100-fold concentration. Aliquots were stored at –80°C. HepaRG cells were stimulated with HBV at 4–100 genome equivalents (GEq)/cell in the presence of 4% PEG8000 (Sigma) for indicated times at 37°C. PHHs were stimulated with HBV at 4–100 GEq/cell with or without the presence of 4% PEG8000 for 24 h at 37°C. At the end of the stimulation period, cells were washed three times with the culture medium and maintained in new medium. A mock "HBV-negative" inoculum was generated by depletion of Dane particles using centrifugal filters devices (Amicon Ultracel 50K; Millipore) and used as a mock control (25).

UV inactivation

HBV was UV irradiated in a UVC 500 UV Crosslinker (Hoefer) for a total dose of 5.94 or 11.88 J/cm² (25).

Reagents

Alpha IFN 2a (IFN- α) was purchased from PBL (Piscataway, NJ) and was used to treat cells for 24 h at 100 U/ml unless otherwise indicated. Polyinosinic:polycytidylic acid [poly(I:C)], poly(deoxyadenylic-deoxythymidylic) [poly(dA:dT)], poly(deoxyguanylic-deoxycytidylic) acid [poly(dG:dC)], and cyclic [G(2',5')pA(3',5')p] (2'3'-cGAMP), obtained from Invivogen (San Diego, CA), were reconstituted in PBS at 1 mg/ml, denatured at 55°C for 30 min, and allowed to anneal at room temperature before use. IFN stimulatory DNA (ISD), which is a 90-bp non-CpG oligomer, was synthesized using following primers: forward primer: 5'-TAC AGA TCT ACT AGT GAT CTA TGA CTG ATC TGT ACA TGA TCT ACA TAC AGA TCT ACT AGT GAT CTA TGA CTG ATC TGT ACA TGA TCT ACA-3'; reverse primer: 5'-TGT AGA TCA TGT ACA GAT CAG TCA TCA TCT ACT AGT AGA TCT GTA TGT AGA TCA TGT ACA GAT CAG TCA TAG ATC ACT AGT AGA TCT GTA-3'. HepaRG, HepG2, Huh 7.5.1, and PHH cells were transfected with 1 μ g poly(I:C), poly(dA:dT), poly(dG:dC), ISD, 2'3'-cGAMP in 3.2 μ l Lipofectamine 2000 (Invitrogen) for 24 h unless otherwise indicated.

IL-28 (detects both IL-28A/IFNL2 and IL-28B/IFNL3) and CXCL10 ELISA kits were purchased from RayBiotech (Norcross, GA). Anti-Actin, anti-cyclic GMP-AMP synthase (cGAS), and anti-IFI16 were purchased from Sigma. Anti-STAT1 was purchased from BD Biosciences. Anti-phospho-STAT1 was purchased from Millipore. Anti-TANK-binding kinase 1 (TBK1), anti-phospho-NF- κ B p65 (Western blot), and NF- κ B p65 (immunofluorescence) Abs were purchased from Cell Signaling. Anti-absent in melanoma 2 was purchased from Novus Biologicals. Anti-I- κ B- α was purchased from Santa Cruz. Anti-human IFN-stimulated gene (ISG) 15 was purchased from PBL Assay Science. BX795 was purchased from Invivogen (San Diego, CA). Entecavir (hydrate) was purchased from Cayman Chemical (Ann Arbor, MI).

RNA interference

Chemically synthesized 21-nt sense and antisense RNA oligonucleotides were obtained from Dharmacon as On Target Plus SMART pools. HepG2 or HepaRG cells were plated on 12-well plates at 250,000 cells/well and transfected with small interfering RNA (siRNA) at a final concentration of 50 nM/well using RNAiMAX (Invitrogen). Assays were typically performed 72 h after siRNA treatment, when gene knockdown was found to be maximal. A negative control (siCONTROL NonTargeting siRNA #2, Dharmacon D-001210–02) was used to account for any off-target effects of the transfected siRNAs.

Microarray analysis

Total RNA was extracted from PHHs with the RNeasy kit from Qiagen according to the manufacturer's instructions. RNA was quantified with a spectrophotometer, and the RNA quality was analyzed with an Agilent bioanalyzer (Agilent Technologies, Palo Alto, CA) according to the manufacturer's instructions. RNA was then amplified with an Agilent Enzo kit. Amplified cRNA was hybridized to an Affymetrix Human 133 Plus 2.0 microarray chip containing 54,675 gene transcripts. The microarray signals were normalized using the robust multiarray average (RMA) algorithm. The significantly expressed genes were selected based on ANOVA analysis by Partek Pro software (Partek, St. Charles, MO). To identify genes in the gene ontology analysis, we used the commercial gene pathway analysis web tool (<http://trials.genego.com/cgi/index.cgi>). The signal values of each probe set ID from the selected gene lists were plotted by the commercial software Partek to generate the heat map. The microarray data can be found using the Gene Expression Omnibus accession number GSE69590 (<http://www.ncbi.nlm.nih.gov/genbank>). Additional information on microarray data analysis is presented later in the *Statistical Analysis* section.

Quantitative PCR

For analysis of endogenous mRNA levels, total RNA was isolated from cells using the RNeasy RNA extraction kit (Qiagen), and cDNA synthesis was performed using 1 μ g total RNA (qScript cDNA Supermix; Quanta Biosciences). Fluorescence real-time PCR analysis was performed using an ABI 7500 instrument (Applied Biosystems, Foster City, CA) and TaqMan gene expression assay (Applied Biosystems). For detection of IFNL2/3, a TaqMan probe that detects both IL-28A/IFNL2 and IL-28B/IFNL3 (FAM Probe CTG CCT CAG GTC CCA, Forward: 5'-CTT TAA GAG GGCCAA AGA TGC-3', Reverse: 5'-CCA GCT CAG CCT CCA AAG-3') was purchased from IDT (Coralville, IA), and the amplicon was confirmed by sequencing analysis to be derived from IFNL2/3. HBV DNA was quantified by real-time PCR analysis using the primer set 5'-ACTCACCAAC-CTCCTGTCT-3' and 5'-GACAAACGGGCAACATACCT-3' and probe 5'-FAM-TATCGCTGGATGTGTCTGCGCGGT-(TAMRA)-3' (26). Detection of covalently closed circular DNA (cccDNA) was achieved using 5'-CGTC-TGTGCTTCTCATCTGC-3' and 5'-GCACAGCTTGGAGGCTTGAA-3' as primers and 5'-CTGTAGGCATAAATTGGT (MGB)-3' as a probe (27). This primer probe set theoretically detected neither relaxed circular DNA nor HBV DNA integrated into host genome but can capture cccDNA as described previously (27). In instances when expression of genes was undetectable, a cycle threshold value of 40 was assigned because this is the limit of detection for this primer-probe set. Relative amounts of mRNA, determined using a FAM-Labeled TaqMan Probe, were normalized to the 18S rRNA levels in each PCR using the eukaryotic 18S rRNA endogenous control from ABI (VIC/MGB Probe, Primer Limited, catalog no. 4319413E). The 2^{–(– δ C_T)} method was used for quantitation of relative mRNA levels and fold induction (28). All other TaqMan probe primers for quantitation of mRNA for target genes were purchased from ABI (Applied Biosystems).

Quantification of HBV DNA

HBV DNA was quantified using COBAS AmpliPrep/COBAS TaqMan HBV test, v2.0 (29). HBV DNA was extracted from the samples with the COBAS AmpliPrep instrument, using the total nucleic acid isolation kit

according to the manufacturer's instructions. Extraction, amplification, and detection steps were performed in batches without the user's intervention. The HBV DNA concentration was automatically calculated by comparing the HBV signal with the HBV quantitation standard for each sample and control. As stated by the manufacturer, the limit of detection was 20 IU/ml. The linear dynamic range of the COBAS AmpliPrep-total nucleic acid isolation-COBAS TaqMan HBV test was 20 to 1.7×10^8 HBV IU/ml. For all values $\geq 1.7 \times 10^8$ HBV IU/ml, it was recommended to retest the sample after dilution if required. The AmpliLink software (Roche Molecular Systems) reported the results as follows: a positive result was considered to be any quantitative value, regardless of the value, or any result < 20 IU/ml. According to the manufacturer's insert, 1 IU is equivalent to 5.82 HBV DNA copies.

Liver biopsy specimens from patients with HBV

Liver biopsy specimens were obtained from patients with chronic hepatitis B or nonalcoholic fatty liver disease (control). A sample of each biopsy specimen was placed in RNeasy (Qiagen) and stored at -80°C until analysis. Total RNA was purified using an RNeasy kit. Hepatic mRNA levels of the target gene were normalized to the level of 18S RNA in each PCR and then plotted relative to the same patient. The $2(-\delta \delta \text{C(T)})$ method was used for quantitation of relative mRNA levels (28). The research protocol used to obtain these samples was approved by the Institutional Review Board, and all patients gave written, informed consent for participation in the study and for the liver biopsy procedure.

Statistical analysis

Data from repeated experiments were averaged and are expressed as means \pm SD. The t test was used for univariate comparisons between patient groups. The p values < 0.05 were considered significant. For microarray experiments, the signal intensity from gene transcripts was compared between treated and untreated samples. Affymetrix CEL files were imported into Partek Genomics Suite 6.3 (Partek, St. Louis, MO) using the default Partek normalization parameters. Probe-level data were preprocessed, including background correction, normalization, and summarization, using RMA analysis. RMA adjusts for background noise on each array using only the perfect match probe intensities, and subsequently normalizes data across all arrays using quantile normalization followed by median polish summarization to generate a single measure of expression. These expression measures were then log-transformed, base 2. ANOVA analysis was performed for comparisons using Partek Pro software (Partek). Before the samples were compared, the signal-to-noise ratio was evaluated by a source of variance analysis. Only genes for which a signal was detected in at least 50% of the samples were included. Expression differences of at least 2.0-fold with $p < 0.05$ were considered significant. Analysis of the data set with Partek using a false discovery rate cutoff of 0.05 yielded similar results. For analysis of human hepatic gene expression, the significance of correlation was assessed using Spearman's rho, using IBM SPSS Statistics version 22 (IBM, Somers, NY). The asterisks indicate $*p < 0.05$, $**p < 0.01$, and $***p < 0.001$.

Results

Upregulation of inflammatory genes by HBV

To determine the biologic role of innate immune responses in the liver to HBV, we used short durations of HBV stimulation. Fig. 1A and 1B demonstrates marked upregulation of chemokines after HBV stimulation of HepaRG cells and PHHs that are known to have functional innate immune responses (2). Increasing GEq per cell used for HBV stimulation resulted in increased upregulation of CXCL10 and CCL5 that increased steadily from 16 to 48 h (Supplemental Fig. 1A, 1B); however, we did not observe significant upregulation of ISG15 and/or STAT1 by Western blot (data not shown). Importantly, we confirmed upregulation of CXCL10 protein by ELISA after stimulation with HBV (Fig. 1C). In addition, treatment with IFN- α was able to decrease levels of both HBV DNA and cccDNA; however, it enabled cells to induce more robust gene induction after stimulation with HBV (Fig. 1D). Similarly, PHHs also induced CXCL10 and CCL5 in response to HBV stimulation, and increasing GEq per cell used for HBV stimulation also correlated with levels of both HBV DNA and cccDNA (Supplemental Fig. 1C, 1D). We also used HepG2 cells expressing the NTCP receptor that supports HBV infection, but we were

unable to demonstrate upregulation of chemokines after HBV stimulation in this cell line with defective innate immune responses; however, IFN demonstrated antiviral activity against HBV as expected (Supplemental Fig. 2A, 2B). In addition, we used UV-inactivated HBV to stimulate HepaRG cells and also observed upregulation, albeit at lower levels, of CXCL10 and CCL5 demonstrating that protein components of the intact virion can contribute to stimulation of hepatocytes (Supplemental Fig. 2C). An additional mock stimulation was performed, utilizing filtrate from our HBV preparation using centrifugal filtration (50-kDa filter) that would remove intact HBV particles but would contain viral or cellular debris including protein and nucleic acid components, with no stimulation being observed. We also confirmed the effectiveness of our UV inactivation in both PHHs and HepG2-NTCP cells (Supplementary Fig. 2D, 2E). To validate our data obtained in vitro, we obtained and analyzed liver biopsies from HBV-infected and uninfected patients. As seen in the in vitro models, levels of CXCL10 and CCL5 were higher in HBV-infected patients, where continuous infection of naive hepatocytes occurs, and there was a significant correlation in levels of these genes indicating concurrent gene induction. In addition, CXCL10 levels correlated with alanine aminotransferase (ALT) levels in HBV-infected patients (Fig. 1E, Supplemental Table 1). To determine whether HBV DNA synthesis and nucleic acid replication is needed to stimulate upregulation of these chemokines, we used entecavir. This small molecule is an effective antiviral agent that inhibits the activity of hepadnaviral polymerases and prevents the formation and continued production of viral replication intermediates. However, we were unable to demonstrate an effect of entecavir on HBV-induced gene expression at early time points pointing to a role for molecular components of the pre-existing virion (Fig. 1F).

To further characterize gene induction by HBV, we performed microarray analysis on HBV-infected PHHs. Fig. 2A demonstrates that there is detectable gene induction of inflammatory cytokines, including CXCL10, after stimulation by HBV. Although CXCL10 was significantly induced, there were many other genes that were induced to a greater level and have yet to be implicated in HBV pathogenesis (Fig. 2B). Pathway analysis performed on this data set demonstrated that there is a marked inflammatory response triggered by HBV (Fig. 2C).

Robust induction of chemokines and IFNL2/3 in response to DNA, poly(dA:dT) and poly(dG:dC), in hepatocytes

Because HBV has a DNA genome and because a recent study has demonstrated that HBV induces type III IFN/IFNL (30), we next investigated the innate immune response and induction of IFNL2/3 mounted after stimulation with dsDNA in human hepatocytes. We initially used dsDNA viral mimetics to stimulate in vitro cell culture models including PHHs and HepaRG cells. As a control, both IFN- α and transfected poly(I:C) were able to upregulate well-characterized viral-stimulated genes that included CXCL10 and IFNL2/3 as previously described (2). Similarly, transfected DNA species such as poly(dA:dT) (b-DNA) and poly(dG:dC) (z-DNA) mounted robust antiviral responses similar to that seen with transfected poly(I:C) (Fig. 3A). We next confirmed upregulation of CXCL10 and IFNL2/3 at the protein level by ELISA (Fig. 3B) and upregulation of ISG15 and STAT1 by Western blot (Fig. 3C). To address the role of the downstream signaling proteins TBK1 and IFN regulatory factor 3 (IRF3) in these models, we first performed experiments studying the ability of poly(dG:dC) and poly(dA:dT) to stimulate IRF3 nuclear translocation using the selective TBK1 inhibitor BX795. As depicted in Fig. 4A, TBK1 is necessary for antiviral responses to poly(dG:dC) and poly(dA:dT) because BX795 blocks nuclear translocation of IRF3. In addition, BX795 also blocks upregulation of CXCL10, radical S-adenosyl methionine domain-containing protein (RSAD2),

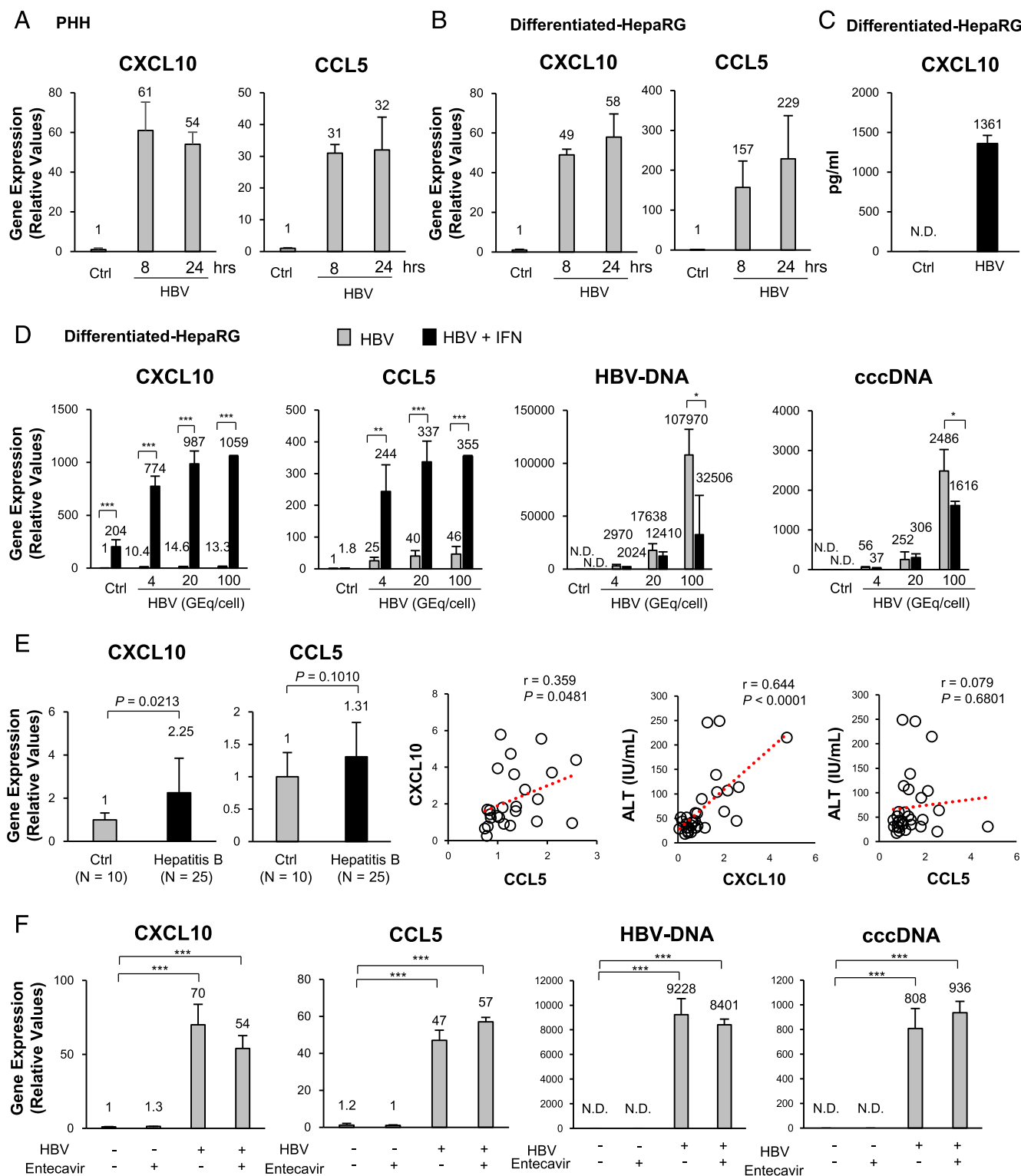


FIGURE 1. Induction of inflammatory genes after stimulation with HBV in hepatocytes. **(A)** qPCR analysis of CXCL10, CCL5 in PHH stimulated with HBV (GEq/cell = 100) for 8 or 24 h relative to 18S rRNA levels. **(B)** qPCR analysis of CXCL10, CCL5 in differentiated HepaRG cells stimulated with HBV (GEq/cell = 100) for 8 or 24 h relative to 18S rRNA levels. **(C)** Analysis of protein production of CXCL10 by ELISA in differentiated HepaRG cells after stimulation with HBV (GEq/cell = 100) for 40 h. **(D)** qPCR analysis of CXCL10, CCL5, HBV DNA, and cccDNA in differentiated HepaRG stimulated with HBV (GEq/cell = 4, 20, 100) for 40 h with or without IFN- α (100 U/ml) relative to 18S rRNA levels. * $p < 0.05$, ** $p < 0.01$, *** $p < 0.001$. **(E)** The mRNA expression levels of CXCL10 and CCL5 in livers of patients with chronic hepatitis B ($n = 25$) and control group ($n = 10$) by qPCR (left two panels). Correlation of CXCL10, CCL5 (relative to 18S rRNA levels) in livers of patients by qPCR and serum ALT levels in patients with chronic hepatitis B ($n = 25$) (right three panels). Dashed lines represent regression; p value represents significance of the Spearman correlation coefficient (p). r = goodness of fit of the regression line. **(F)** Differentiated HepaRG cells were pretreated with 100 ng/ml entecavir for 2 h and then incubated with HBV (GEq/cell = 100) for 16 h. After incubation of HBV for 16 h, cells were washed three times with media and cultured with virus-free entecavir-containing medium for 24 h for a total virus stimulation time of 40 h. mRNA levels of CXCL10, CCL5, HBV-DNA, and cccDNA in differentiated HepaRG cells were quantitated by quantitative RT-PCR. *** $p < 0.001$. N.D., not detected.

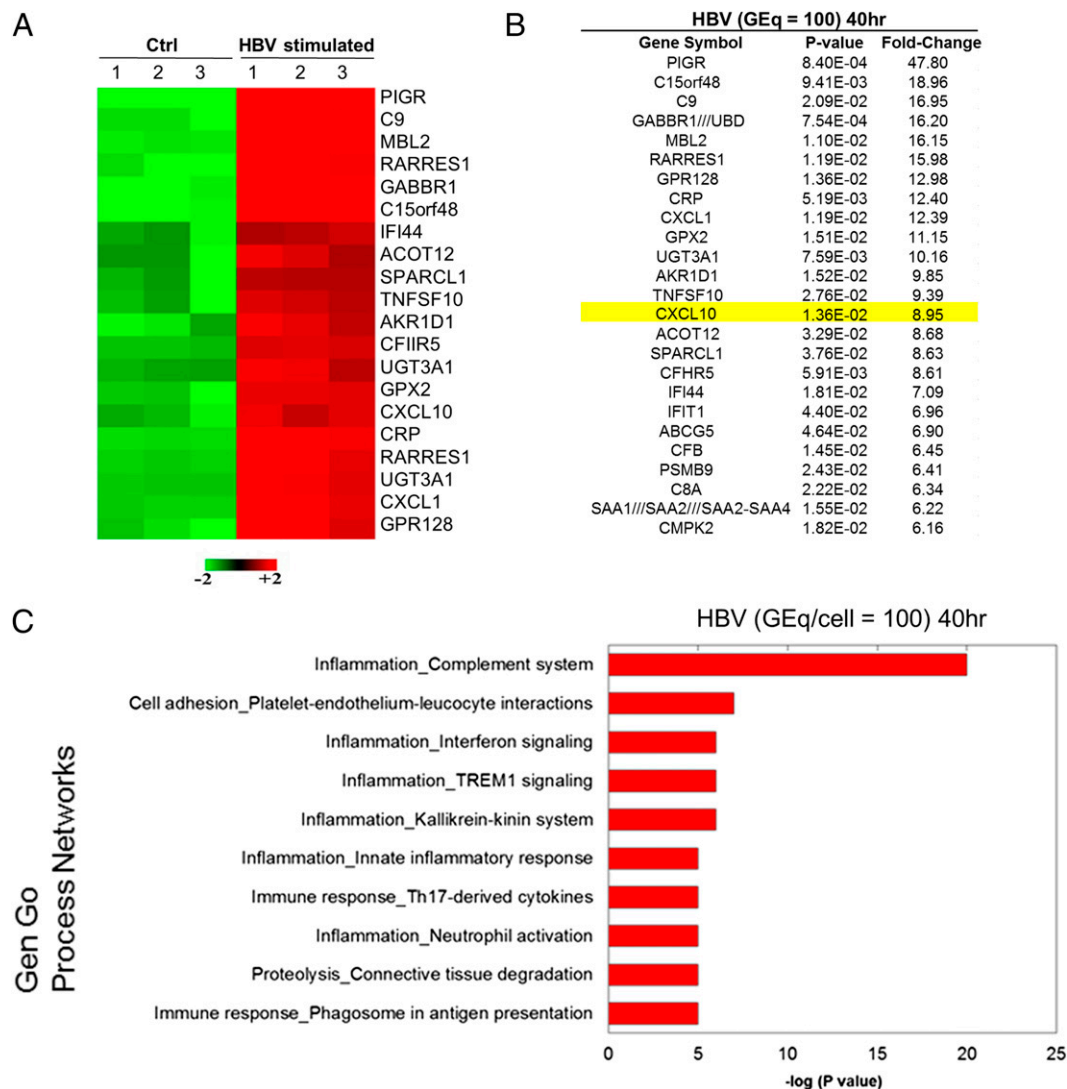


FIGURE 2. Microarray analysis of PHHs stimulated with HBV. PHHs were stimulated with HBV (GEq/cell = 100) for 40 h. **(A)** Heat maps generated using microarray data from three replicates (three mock-treated control and three HBV-stimulated PHH samples from the same donor). **(B)** Top 26 genes ranked by fold induction after stimulation with HBV. **(C)** GeneGo networks that are significantly upregulated after stimulation with HBV.

and IL-28 at the mRNA level (Fig. 4B). siRNA-mediated down-regulation of TBK1 also proved to be effective in blocking up-regulation of these genes by poly(dG:dC) and poly(dA:dT) (Fig. 4C).

Robust induction of chemokines in response to DNA, ISD, and 2'3'-cGAMP in hepatocytes

Recently, additional pathogen DNA mimetics including ISD and 2'3'-cGAMP have been shown to stimulate robust innate immune responses in transfected cells (31, 32). To examine the effect of these DNA mimetics, we first used the HepaRG cell line that has intact antiviral signaling pathways. Fig. 5A demonstrates that transfected ISD is able to induce IRF3 translocation, suggesting that HepaRG cells can be stimulated by ISD to mount an antiviral response. ELISA analysis in both PHHs and HepaRG cells demonstrated the ability of both ISD and 2'3'-cGAMP to produce only CXCL10 24 h after stimulation, but not IFNL2/3 protein (Fig. 5B), unlike poly(dA:dT) and poly(dG:dC) (Fig. 4B). Fig. 5C also shows that ISD and 2'3'-cGAMP are able to induce ISG15 by Western blot and CXCL10 and RSAD2 at the RNA level (Fig. 5D). However, we were unable to detect phosphorylation of STAT1 after 6 h of stimulation with the transfected ISD and 2'3'-cGAMP, whereas both poly(dA:dT) and poly(dG:dC) did so as determined by Western blot

analysis (Fig. 5E). Interestingly, phosphorylation of STAT1 was observed after 24 h of stimulation with transfected ISD and 2'3'-cGAMP (Fig. 5E), demonstrating a delay in activation of STAT1 when compared with poly(dA:dT) and poly(dG:dC).

Transfected dsDNA results in a distinct pattern of gene expression

Having validated the upregulation of CXCL10 at the mRNA and protein levels, we next examined the global gene expression after transfection of ISD into PHHs at 12 and 24 h posttransfection to provide additional information on the upregulation of the IFNs and other antiviral genes in hepatocytes. We identified genes that showed significant changes after transfection of ISD using a cutoff of $p < 0.05$ and fold change > 2.0 (Fig. 6), as well as with a false discovery rate cutoff of 0.05 (data not shown). The results shown in the heat map of Fig. 6A illustrate the broad range of changes in the transcriptome that occur after transfection of dsDNA into PHHs that increased over time (Fig. 6B).

Using pathway analysis, we identified various biological processes that were overrepresented by genes whose expression levels were significantly affected after transfection of ISD (Fig. 6C). RSAD2 and CXCL10, which were confirmed to be upregulated by quantitative

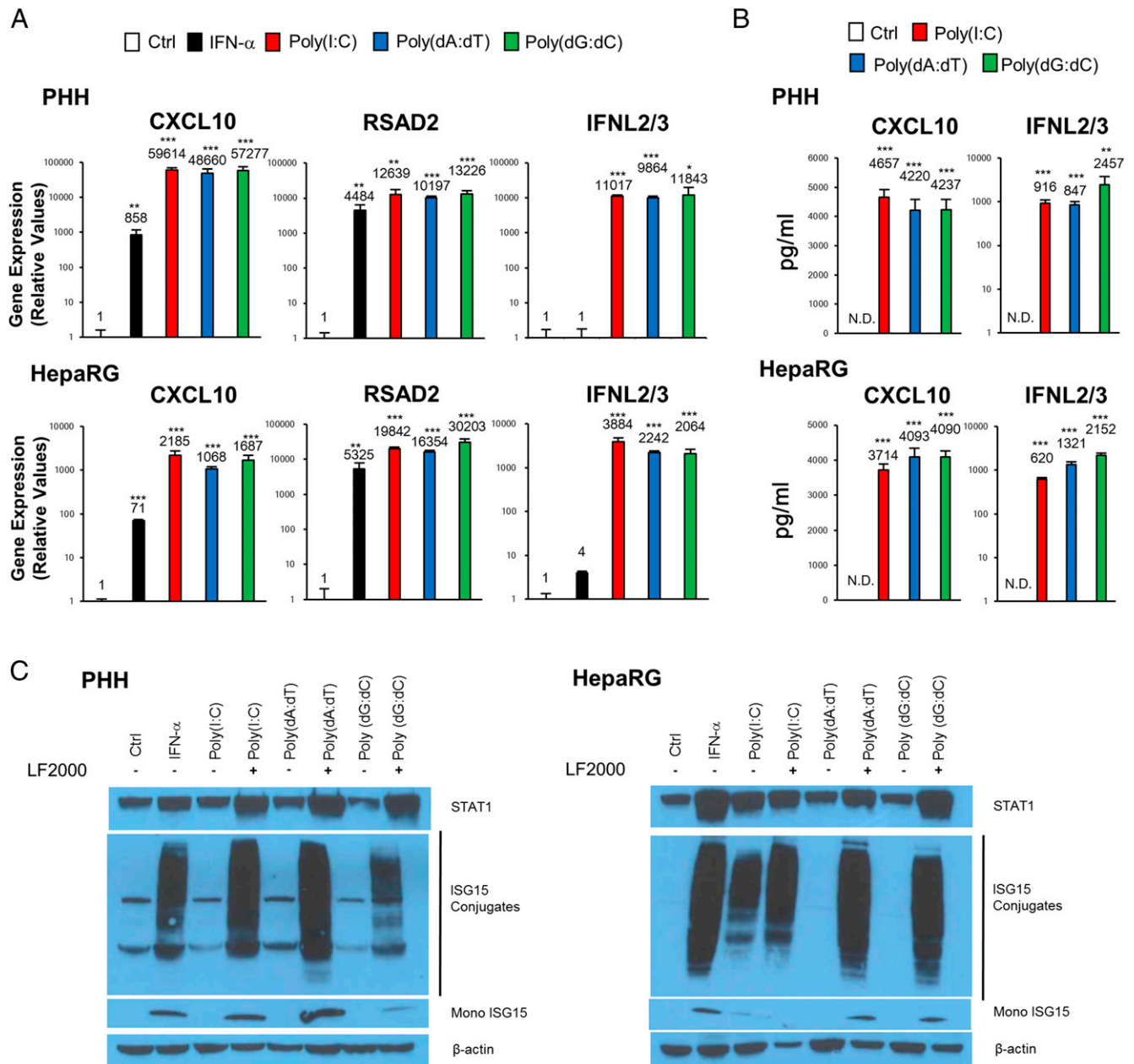


FIGURE 3. Activation of RNA-stimulated antiviral pathways after treatment with DNA in hepatocytes. **(A)** Analysis of CXCL10, RSAD2, and IFNL2/3 mRNA levels by qPCR in PHHs and HepaRG cells after treatment with IFN- α (100 U/ml) or transfection with 1 μ g/ml poly(I:C), poly(dA:dT), or poly(dG:dC) for 24 h relative to 18S rRNA levels. **(B)** Analysis of protein production of CXCL10 and IFNL2/3 by ELISA in PHHs and HepaRG cells after transfection with 1 μ g/ml poly(I:C), poly(dA:dT), or poly(dG:dC) for 24 h. **(C)** Western blot analysis of STAT1, ISG15, and β -actin on protein lysates from PHHs and HepaRG cells after treatment with IFN- α (100 U/ml) or 1 μ g/ml poly(I:C), poly(dA:dT), or poly(dG:dC) for 24 h. Lipofectamine 2000 (LF2000) was used as indicated. * p < 0.05, ** p < 0.01, *** p < 0.001, in comparison with control group. N.D., not detected.

PCR (qPCR) (Fig. 5D), were among the top 20 genes upregulated (ranked by fold induction) in the transfected cells (Fig. 6D). Comparison of the genes induced at 12 versus 24 h demonstrated that with time, ISD increases the level of mRNA upregulation including CCL5. To further confirm these changes in induction of antiviral genes by ISD, a time-course and dose-dependency study was conducted (Supplemental Fig. 3A). Similar results were obtained from cells transfected with 2'3'-cGAMP (Supplemental Fig. 3B).

Role of known DNA-sensing pathways in innate immune responses to HBV in hepatocytes

To further address the mechanisms by which ISD can induce antiviral gene signaling in hepatocytes, we begin by studying proteins

that have been demonstrated to have a role in foreign DNA-sensing because most demonstrate tissue-specific expression. Gamma IFN inducible protein 16 (IFI16), a known DNA sensor (33), was found to be absent in hepatoma cells lines except HepaRG cells (Supplemental Fig. 3C). After inducing a marked decrease in IFI16 protein levels using siRNA, we were unable to observe any role for this protein in the upregulation of CXCL10 and RSAD2 by transfected ISD (Supplemental Fig. 3D). We next investigated the role of absent in melanoma 2, another known DNA signaling molecule (34), and similarly observed little effect on ISD-stimulated gene induction (Supplemental Fig. 3E, 3F).

To further investigate the recognition of foreign DNA in hepatocytes, we also examined the stimulator of IFN genes (STING)

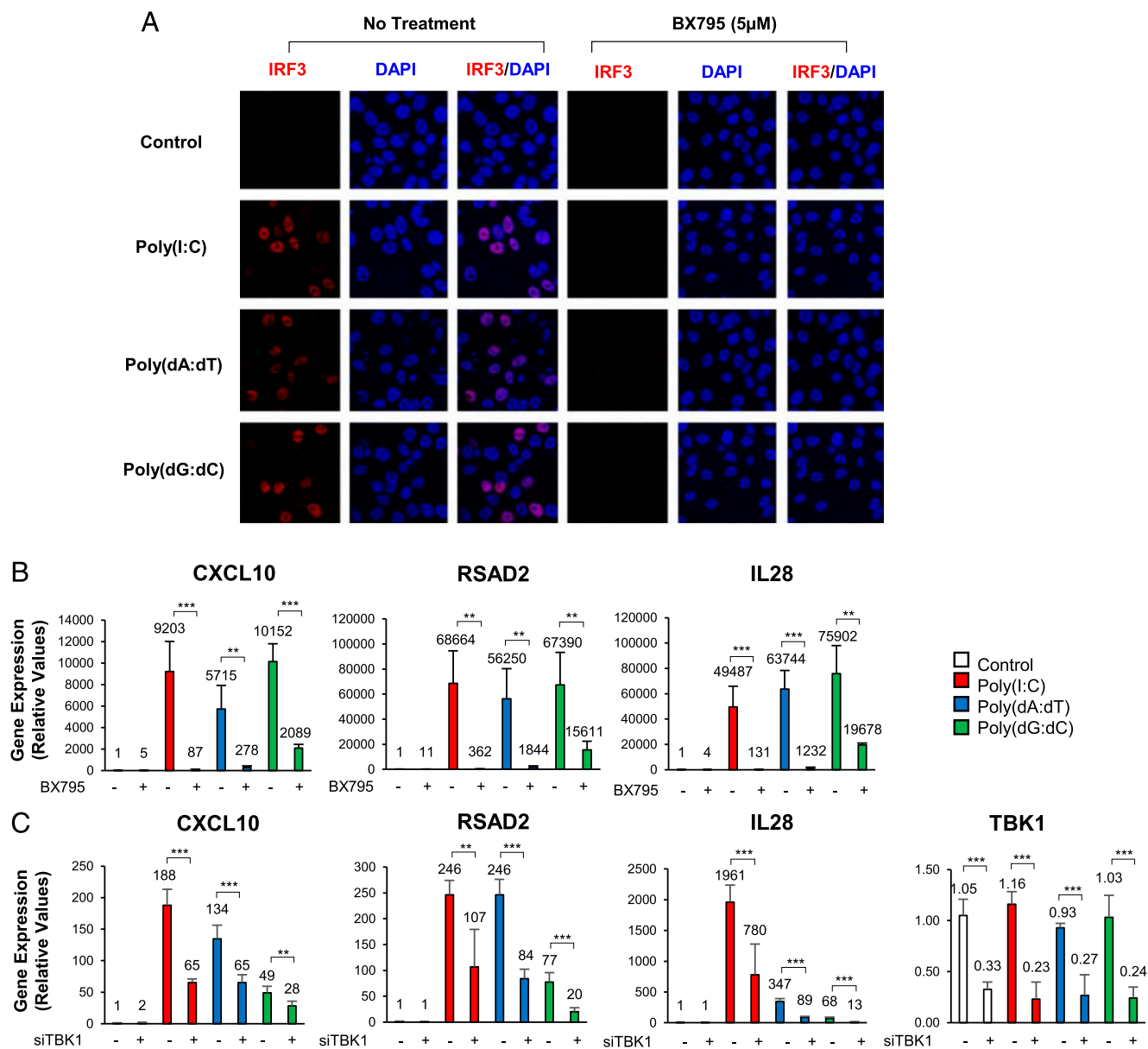


FIGURE 4. Role of TBK1 in signaling after stimulation with poly(dA:dT) or poly(dG:dC) determined by IRF3 translocation or qPCR. **(A)** Immunofluorescence microscopy analysis of IRF3 nuclear localization (red) and nuclear staining of DAPI (blue) in HepaRG cells after transfection with 1 μ g/ml poly(I:C), poly(dA:dT), or poly(dG:dC) for 24 h with Lipofectamine 2000. BX795, a selective TBK1 inhibitor, was added at a final concentration of 5 μ M for 6 h before the transfection. Original magnification $\times 40$. **(B)** qPCR analysis of CXCL10, RSAD2, and IL-28 gene expression in HepaRG cells after transfection of 1 μ g/ml poly(I:C), poly(dA:dT), or poly(dG:dC) for 24 h in the presence or absence of TBK1 inhibitor BX795 (5 μ M). **(C)** qPCR analysis of CXCL10, RSAD2, IL28, and TBK1 gene expression in HepaRG cells, which were treated with siRNA against nontargeting control or TBK1 for 72 h before stimulation with 1 μ g/ml poly(I:C), poly(dA:dT), or poly(dG:dC) for 5 h. All transfections were performed using Lipofectamine 2000. * $p < 0.05$, ** $p < 0.01$, *** $p < 0.001$.

pathway that has been shown to be important for DNA responses and innate responses to HBV (17, 35, 36). Interestingly, knockdown of STING and the associated molecule cGAS and downstream proteins TBK1 and IRF3 had dramatic effects on gene induction by ISD, demonstrating almost complete inhibition (Fig. 7A–D). We next addressed the role of NF- κ B by targeting I κ B kinase γ (IKK γ)/NEMO using siRNAs or using a chemical inhibitor targeting the IKK complex (BMS-345541), and we also observed a decrease in gene upregulation (Fig. 7E, 7F).

To determine the signaling pathways involved in HBV-induced gene induction, we used siRNA to target the previous pathways that were interrogated for their role in DNA signaling. Interestingly, most of them did not play a significant role in chemokine induction

(Fig. 8A). However, NF- κ B signaling proved to be important for gene induction by HBV as demonstrated by experiments using siRNAs targeting IKK γ (Fig. 8B). Furthermore, through the use of a chemical inhibitor of the IKK complex (BMS-345541), which blocks NF- κ B signaling, we validated this pathway to be important for chemokine upregulation in both HepaRG cells (Fig. 8C) and PHHs (Fig. 8D). In line with this result, HBV stimulation of HepaRG cells and PHHs resulted in dramatic activation of the NF- κ B pathway as demonstrated by significant induction of phospho-p65 and degradation of I κ B- α as seen by Western blot (Fig. 8E), and activation of p65/nuclear translocation was confirmed through confocal microscopy at very early time points (Fig. 8F).

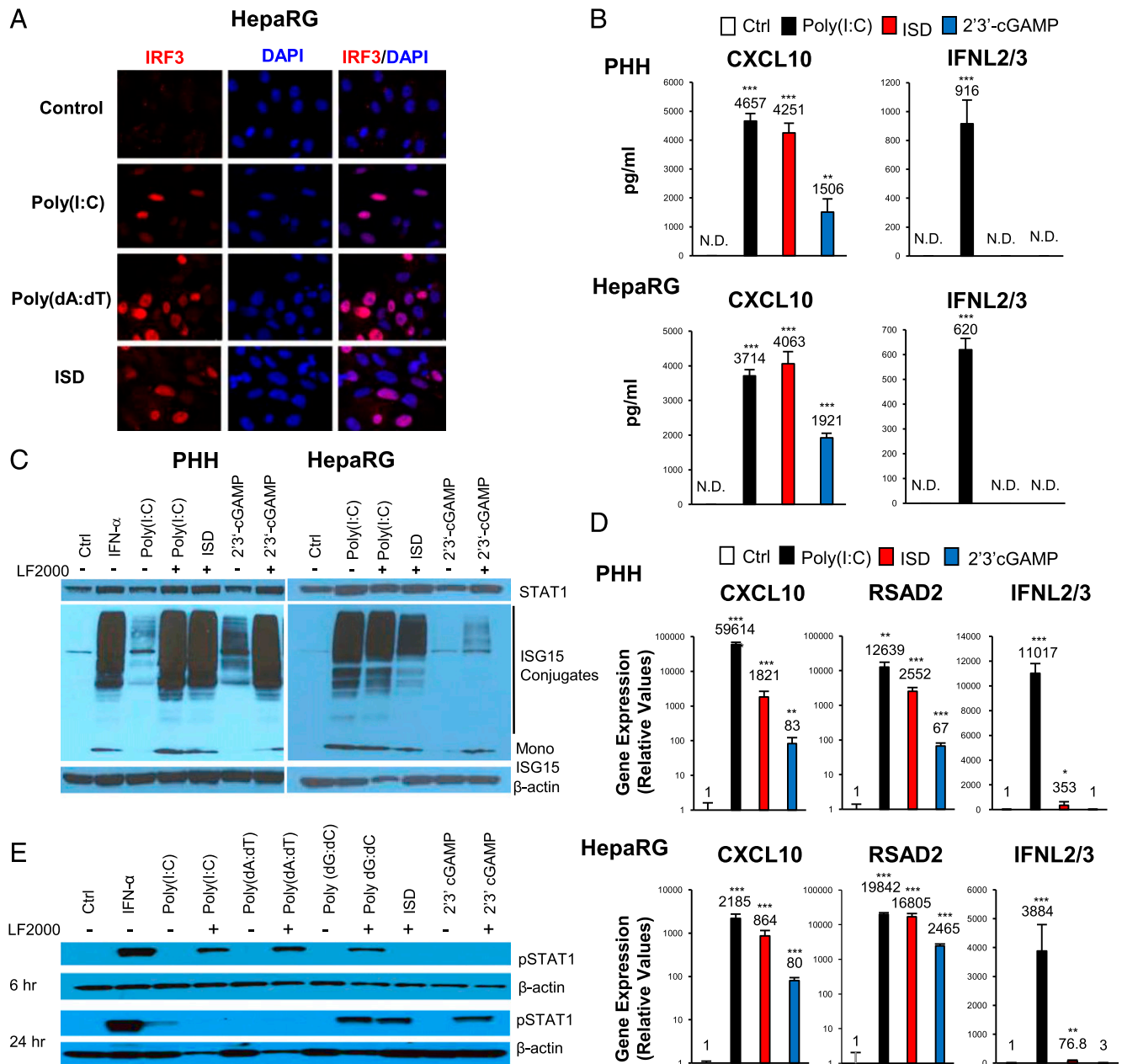


FIGURE 5. Activation of RNA-independent antiviral pathways after treatment with DNA in hepatocytes. **(A)** Immunofluorescence of IRF3 (red) and DAPI (blue) in HepaRG cells after transfection with 1 μ g/ml poly(I:C), poly(dA:dT), or ISD for 24 h. Original magnification $\times 40$. **(B)** Analysis of protein production of CXCL10 and IFNL2/3 by ELISA in PHHs and HepaRG cells after transfection with 1 μ g/ml poly(I:C), ISD, or 2'3'-cGAMP for 24 h. **(C)** Western blot analysis of STAT1, ISG15, and β -actin on protein lysates from PHHs and HepaRG cells after treatment with IFN- α (100 U/ml), 1 μ g/ml poly(I:C), ISD, or 2'3'-cGAMP for 24 h. Lipofectamine 2000 (LF2000) was used as indicated. **(D)** Analysis of CXCL10, RSAD2, and IFNL2/3 mRNA levels by qPCR in PHHs and HepaRG cells after treatment with 1 μ g/ml poly(I:C), ISD, or 2'3'-cGAMP for 24 h relative to 18S rRNA levels. **(E)** Western blot analysis of phosphorylation of STAT1 and β -actin from HepaRG cell lysates after treatment with IFN- α (100 U/ml) or 1 μ g/ml poly(I:C), poly(dA:dT), poly(dG:dC), ISD, or 2'3'-cGAMP for 6 or 24 h. Lipofectamine 2000 (LF2000) was used as the transfection reagent as indicated. * $p < 0.05$, ** $p < 0.01$, *** $p < 0.001$, in comparison with control group. N.D., not detected.

Further experiments were conducted to identify additional genes involved in sensing of HBV infection. We had noticed that HBV-induced gene upregulation was increased when cells were also treated with IFN- α (Figs. 1D, 9A), and this occurred for CCL5 that is a minimally IFN-induced gene (2). Therefore, we surmised that an ISG was involved in sensing of HBV. Because HBV produces a pregenomic RNA species from its DNA genome during its viral life cycle and HBV virions contain viral RNAs (5), we determined the role of two RNA sensors, melanoma differentiation-associated gene 5 (MDA5) and retinoic acid-inducible gene (RIG-I), which are known ISGs involved indirectly in recognition of DNA through

the activity of cellular RNA polymerases and are also induced by HBV stimulation at early time points (Fig. 9B). Surprisingly, siRNA-mediated knockdown of MDA5 had a dramatic effect on HBV gene upregulation that was much stronger than the effect of RIG-I knockdown (Fig. 9C, 9D). Interestingly, downregulation of MDA5 resulted in increased levels of intracellular HBV DNA, cccDNA, and extracellular HBV DNA (Fig. 9E) that was not observed with knockdown of RIG-I (data not shown). To further investigate our data obtained in vitro, we analyzed liver biopsies from HBV-infected and uninfected patients. As seen in the in vitro models, both MDA5 and RIG-I are expressed, as determined by

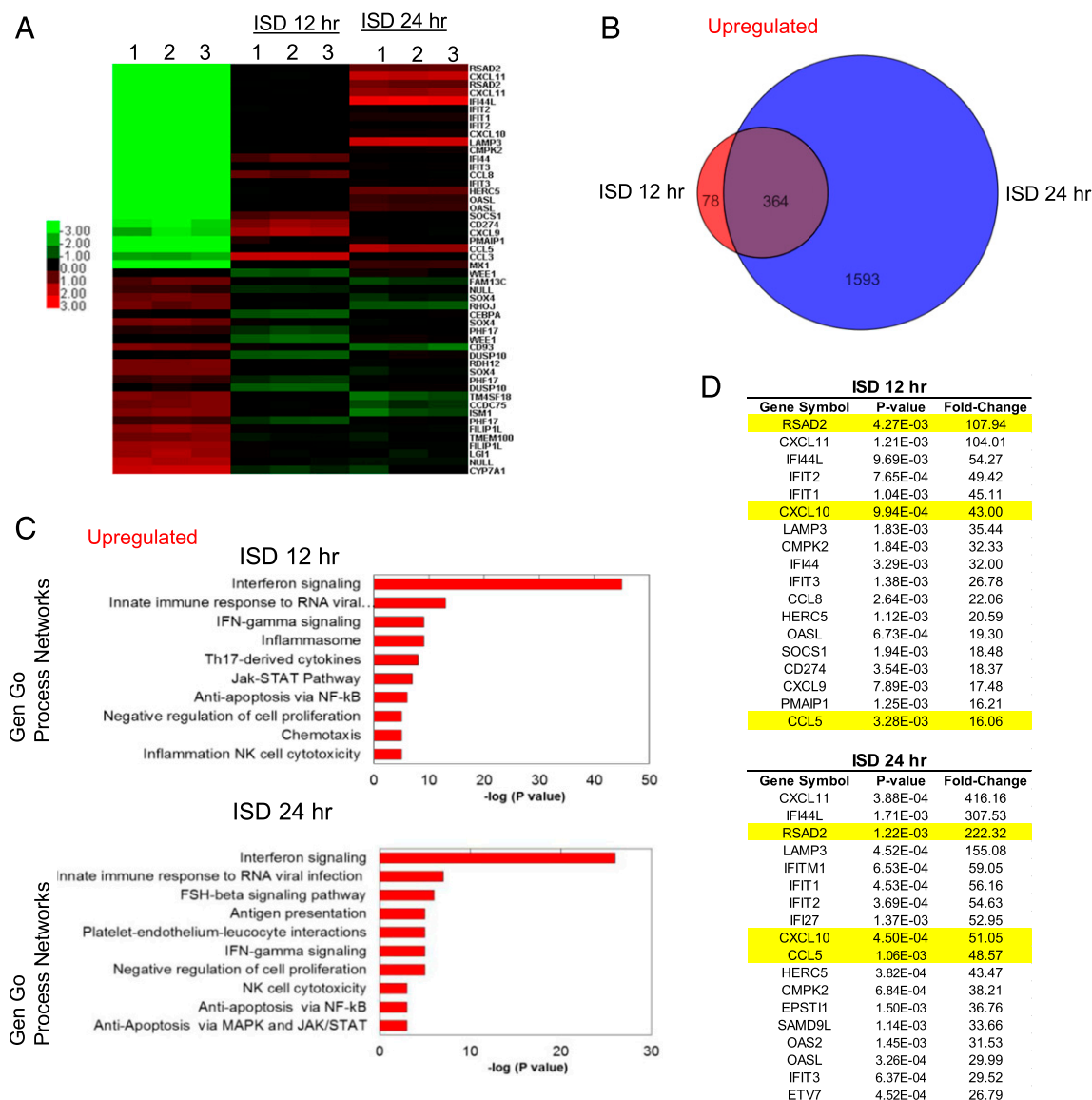


FIGURE 6. Microarray analysis of PHHs transfected with ISD. PHHs were transfected with 1 μ g/ml ISD for the indicated time points. **(A)** Heat maps generated using microarray data from three replicates (12 or 24 h treatment.). **(B)** Venn diagrams displaying the number of probe sets upregulated (>2.0 -fold change) after treatment with ISD for 12 or 24 h. **(C)** GeneGo networks that are significantly upregulated after treatment with ISD for 12 or 24 h. **(D)** Top 18 genes ranked by fold induction after treatment with ISD for 12 or 24 h.

qPCR, but they were not significantly upregulated in our patient samples and there was not a correlation with either gene and ALT as presented in Fig. 9F and 9G. However, as shown in Fig. 9B, MDA5 and RIG-I are expressed in hepatocytes and with IFN treatment, we believe that MDA5 and RIG-I are strongly upregulated and contribute more to the antiviral response to HBV. In addition, as shown in Fig. 9H, both MDA5 and RIG-I mRNA levels demonstrate the highest correlation in expression demonstrating similar gene regulation. In addition, both MDA5 and RIG-I expression levels are significantly correlated to CCL5 gene expression. We did not observe a significant correlation between MDA5 and RIG-I expression levels and CXCL10 gene expression. However, there appears to be a trend supporting a correlation between MDA5 and CXCL10 that is more significant than that between RIG-I and CXCL10 (Fig. 9H). This supports a stronger link between MDA5 and the expression levels of CXCL10 when compared with RIG-I, and the roles of MDA5 and RIG-I in HBV innate immune responses are outlined in Fig. 10.

Discussion

In patients and chimpanzees infected with HBV, previous studies have been unable to demonstrate a robust intrinsic innate immune response (7) that can be seen with other hepatitis viruses such as HCV (2), even though HBV can replicate to very high levels in patients. However, several published studies have recently investigated and characterized HBV infection in vitro models and have provided evidence for activation of innate immune pathways (25, 30). We therefore endeavored to investigate this by focusing on very early time points after simulation with HBV and DNA-driven innate immune pathways that may play a role in HBV infection. We reproducibly demonstrate that foreign DNA and HBV can stimulate innate immune responses in hepatocytes in multiple models and have used several controls to rule out the possibility of stimulation arising from contaminants in the viral preparation.

In this study, we used DNA mimetics that are known to result in the activation of RNA pathways and the RNA mimetic poly(I:C) as

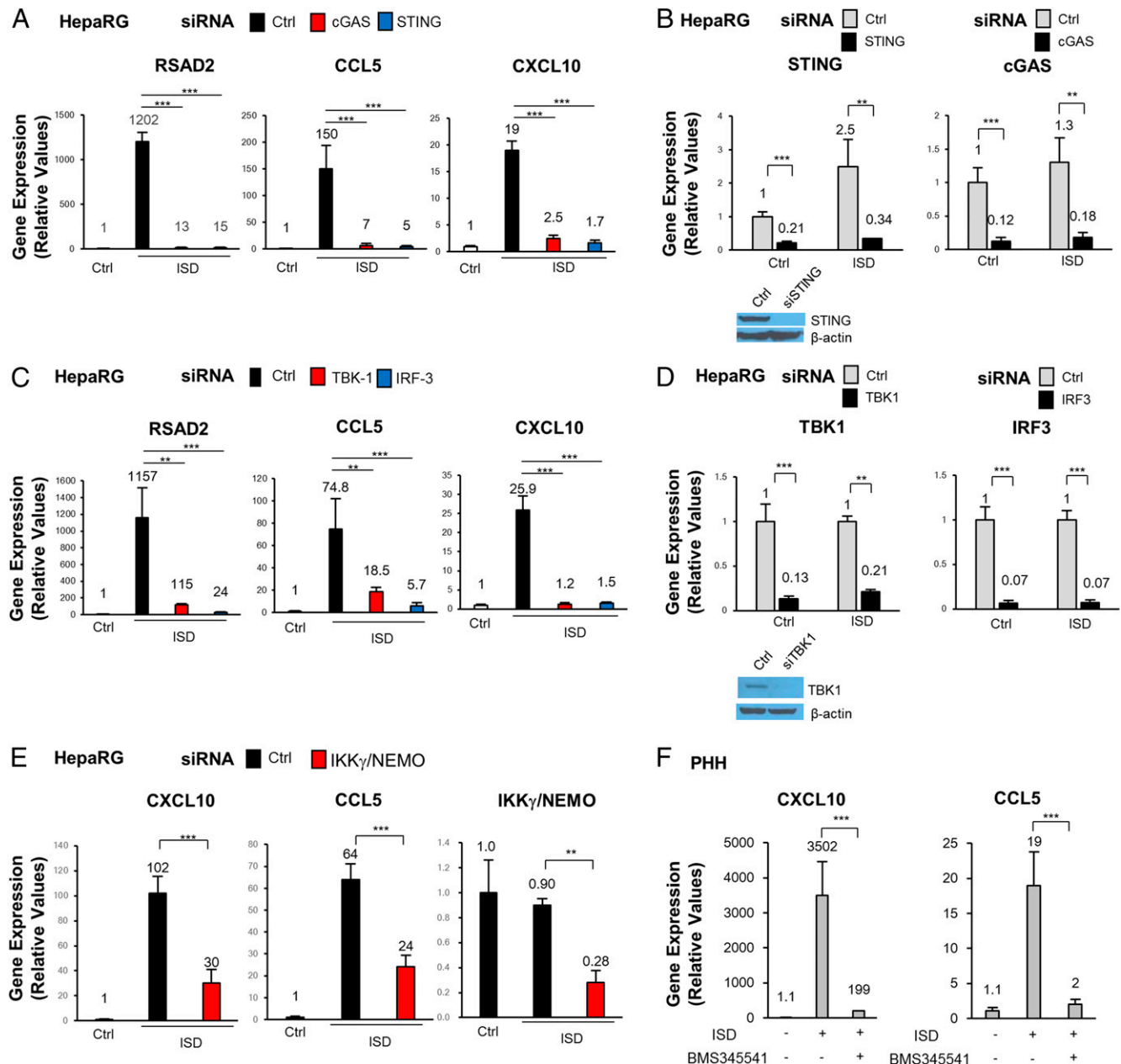


FIGURE 7. Induction of inflammatory genes by ISD is mediated through signaling pathways involving cGAS, STING, TBK1, IRF3, and NF- κ B in hepatocytes. **(A)** qPCR analysis of RSAD2, CCL5, and CXCL10 in HepaRG cells first treated with siRNA for 3 d targeting cGAS or STING and then transfected with 1 μ g/ml ISD for 24 h relative to 18S rRNA levels. Nontargeting siRNA represents control. **(B)** qPCR analysis of STING or cGAS in HepaRG cells first treated with siRNA for 3 d targeting cGAS or STING and then transfected with 1 μ g/ml ISD for 24 h. Western blot of STING and β -actin after treatment with siRNA for 3 d targeting STING relative to 18S rRNA levels. Nontargeting siRNA represents control. **(C)** qPCR analysis of RSAD2, CCL5, and CXCL10 in HepaRG cells first treated with siRNA for 3 d targeting TBK-1 or IRF3 and then transfected with 1 μ g/ml ISD for 24 h relative to 18S rRNA levels. Nontargeting siRNA represents control. **(D)** qPCR analysis of TBK-1 or IRF3 in HepaRG cells first treated with siRNA for 3 d targeting TBK-1 or IRF3 and then transfected with 1 μ g/ml ISD for 24 h. Western blot of TBK-1 and β -actin expression after treatment with siRNA for 3 d targeting TBK-1 relative to 18S rRNA levels. Nontargeting siRNA represents control. **(E)** qPCR analysis of CXCL10, CCL5, and IKK γ /NEMO in HepaRG cells first treated with siRNA for 3 d targeting IKK γ /NEMO and then transfected with 1 μ g/ml ISD for 24 h relative to 18S rRNA levels. Nontargeting siRNA represents control. **(F)** qPCR analysis of CXCL10, CCL5 in PHHs incubated with 10 μ M BMS-345541 and transfected with 1 μ g ISD for 24 h relative to 18S rRNA levels. ** p < 0.01, *** p < 0.001.

a control. Through these experiments, we discovered that certain DNA mimetics including poly(dG:dC) and poly(dA:dT), when transfected, are potent stimulators of IFNL2/3 production and corresponding activation of STAT1 through phosphorylation at early time points. This production of IFNL2/3 occurs mainly through TBK1 and IRF3 in hepatocytes.

To extend these studies, we then used DNA mimetics that stimulate antiviral responses independent of an RNA intermediary.

Interestingly, stimulation with transfected ISD and 2'3'-cGAMP resulted in significant production of CXCL10 at both the mRNA and the protein level. However, IFNL2/3 was not detected at the protein level, alluding to the possibility that RNA-independent DNA-sensing pathways do not result in secretion of IFNL2/3 at early time points. To characterize this RNA-independent DNA-stimulated pathway further in hepatocytes, we then used microarray analyses to characterize the transcriptional profile induced

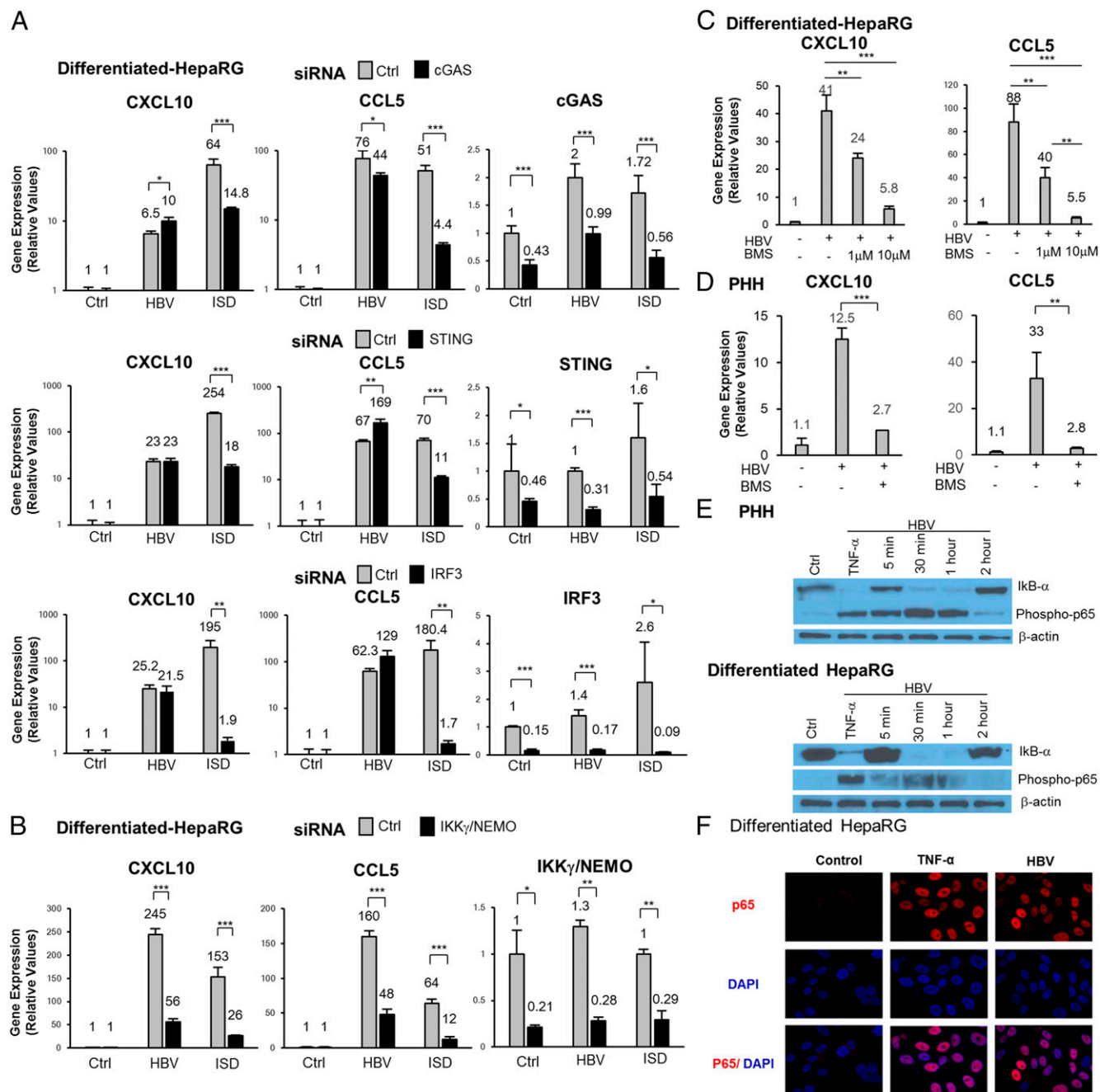


FIGURE 8. Induction of inflammatory genes by HBV is mediated through signaling pathways involving NF- κ B. **(A)** qPCR analysis of CXCL10, CCL5, cGAS, STING, and IRF3 in differentiated HepaRG cells first treated with siRNA for 3 d targeting cGAS, STING, or IRF3 and then stimulated with HBV (GEq/cell = 100) for 40 h or treated with 1 μ g/ml ISD for 24 h relative to 18S rRNA levels. Nontargeting siRNA represents control. **(B)** qPCR analysis of CXCL10, CCL5, or IKK γ /NEMO in differentiated HepaRG cells first treated with siRNA for 3 d targeting IKK γ /NEMO and then stimulated with HBV (GEq/cell = 100) for 40 h or treated with 1 μ g/ml ISD for 24 h relative to 18S rRNA levels. Nontargeting siRNA represents control. **(C)** qPCR analysis of CXCL10 and CCL5 in differentiated HepaRG cells incubated with BMS-345541 (1 or 10 μ M) and stimulated with HBV (GEq/cell = 100) for 40 h relative to 18S rRNA levels. **(D)** qPCR analysis of CXCL10 and CCL5 in PHHs incubated with 10 μ M BMS-345541 and stimulated with HBV (GEq/cell = 100) for 40 h relative to 18S rRNA levels. **(E)** Western blot analysis of I κ B- α , phospho-p65, and β -actin on protein lysates from differentiated HepaRG or PHHs. HepaRG or PHHs were incubated with 2 ng/ml TNF- α for 30 min or stimulated with HBV (5 min, 30 min, 1 h, or 2 h). **(F)** Immunofluorescence of p65 (red) and DAPI (blue) in differentiated HepaRG cells after incubation with 2 ng/ml TNF- α or stimulation with HBV (GEq/cell = 100) for 1 h. Original magnification $\times 40$. * p < 0.05, ** p < 0.01, *** p < 0.001.

by ISD in PHHs. It was evident that a robust inflammatory response was triggered with transfection of ISD. Pathway analysis of the microarray data was also informative as additional insight was gained into the effects of transfected ISD on the transcriptome. Surprisingly, when the top 20 upregulated genes are examined, both type I and III IFNs are absent in ISD-stimulated cells, whereas the type III IFNs are among the top 5 genes stimulated by HCV (2).

Through the utilization of siRNAs targeting several DNA sensors, we were able to confirm the importance of the STING-TBK1-IRF3 pathway in the recognition of ISD in hepatocytes. In addition, NF- κ B also played an important role in upregulation of CXCL10 and CCL5 by ISD.

Through the use of in vitro models of HBV stimulation, we observed upregulation of CXCL10, mRNA and protein, and CCL5

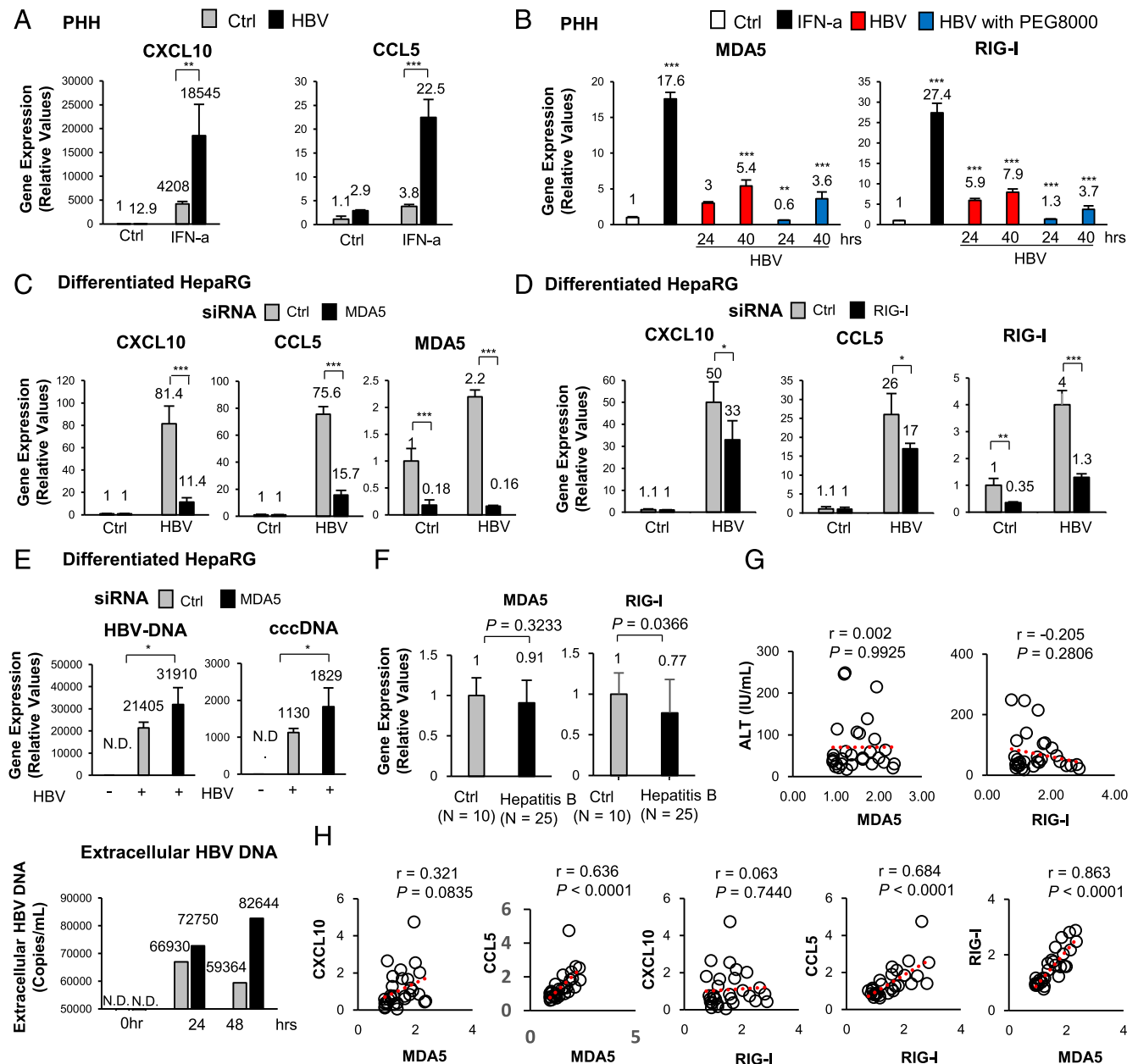
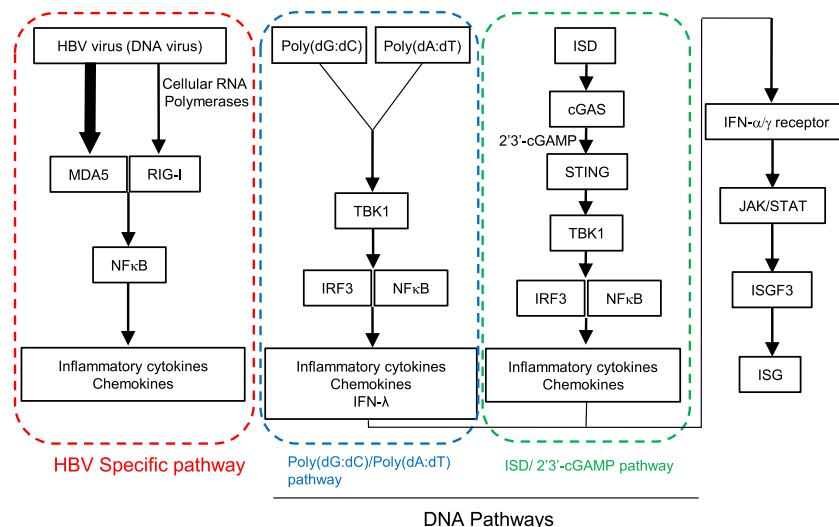


FIGURE 9. HBV stimulation induces cytokine upregulation through the IFN-induced genes MDA5 and RIG-I. **(A)** qPCR analysis of CXCL10, CCL5 in PHHs stimulated with HBV (GEq/cell = 100) for 40 h with or without IFN- α (100 U/ml) relative to 18S rRNA levels. **(B)** qPCR analysis of MDA5 and RIG-I in PHH stimulated with HBV (GEq/cell = 100) for 24 or 40 h with or without using PEG8000 relative to 18S rRNA levels. **(C)** qPCR analysis of CXCL10, CCL5, and MDA5 in differentiated HepaRG cells first treated with siRNA for 3 d targeting MDA5 and then stimulated with HBV (GEq/cell = 100) for 40 h. Nontargeting siRNA represents control relative to 18S rRNA levels. **(D)** qPCR analysis of CXCL10, CCL5, and RIG-I in differentiated HepaRG cells first treated with siRNA for 3 d targeting RIG-I and then stimulated with HBV (GEq/cell = 100) for 40 h relative to 18S rRNA levels. Nontargeting siRNA represents control. **(E)** qPCR analysis of HBV DNA (top left) and cccDNA (top right) in differentiated HepaRG cells first treated with siRNA for 3 d targeting MDA5 and then stimulated with HBV (GEq/cell = 100) for 40 h relative to 18S rRNA levels. Nontargeting siRNA represents control. Twenty-four and forty-eight hours after washing HBV-stimulated HepaRG cells (total 40 and 64 h from the beginning of HBV incubation), medium was collected and extracellular HBV DNA was measured (bottom panel). **(F)** The mRNA expression levels of MDA5 and RIG-I in livers of patients with chronic hepatitis B ($n = 25$) and control group ($n = 10$) by qPCR. Correlation of MDA5 and RIG-I (relative to 18S rRNA levels) in livers of patients by qPCR analysis. **(G)** Serum ALT levels in patients with chronic hepatitis B ($n = 25$) (right two panels). Dashed lines represent regression; p value represents significance of the Spearman correlation coefficient (p). r = goodness of fit of the regression line. **(H)** Correlation of CXCL10, CCL5, MDA5, and RIG-I (relative to 18S rRNA levels) by qPCR in livers of patients with chronic hepatitis B ($n = 25$) (right two panels). Dashed lines represent regression; p value represents significance of the Spearman correlation coefficient (p). r = goodness of fit of the regression line. * $p < 0.05$, ** $p < 0.01$, *** $p < 0.001$.

at very early time points. We were unable to detect upregulation of IFNL2/3 protein with our sensitive assays that are able to detect both upregulation of IFNL2/3 mRNA and protein secretion post HCV infection (2). Indeed, these observations were confirmed in patient liver biopsies, where new hepatocytes are constantly being infected, with both CXCL10 and CCL5 upregulation observed and

their levels correlating with each other. In addition, stimulation with both ISD and 2'3'-cGAMP triggered gene induction that increased with time, whereas HBV-induced genes increased at early time points and then subsequently decreased slightly. It is therefore possible that the HBV virion possesses the ability to downregulate inflammatory gene induction through unknown mechanisms and

FIGURE 10. Proposed model that highlights the role of nucleic acid signaling in intrinsic innate immunity in the liver. First, HBV stimulates the cell, and HBV is sensed by the IFN-induced genes MDA5 and RIG-I, leading to activation of NF- κ B and resulting in production of inflammatory genes including CXCL10. IFNL2/3 protein is not significantly induced as is CXCL10. Second, transfected poly(dG:dC) activates TBK1 leading to activation of IRF3 resulting in production of inflammatory cytokines and IFNL2/3 protein. Third, transfected poly(dA:dT) activates TBK1 leading to activation of IRF3, resulting in production of inflammatory cytokines and IFNL2/3. Fourth, DNA mimetics, transfected into cells, such as ISD and 2'3' cGAMP, bind cGAS and STING, leading to activation of IRF3 producing inflammatory cytokines such as CXCL10, but not significant amounts of IFNL2/3 protein, at early time points.



these may contribute to the previous description of HBV as a stealth virus. Indeed, we were unable to demonstrate upregulation of the known ISGs MDA5 and RIG-I in HBV-infected patient liver biopsies.

We also explored changes in the transcriptome after stimulation with HBV in PHHs. When compared with cells treated with ISD, it is apparent that HBV stimulates a stronger inflammatory response as opposed to an antiviral IFN response. As expected, CXCL10 was among the top genes upregulated by HBV stimulation; however, many genes are upregulated in this data set that have not been associated with HBV infection before. It is evident that inflammatory pathways are significantly stimulated in contrast with that observed post HCV infection where IFN pathways are most activated (2). Future interrogation of this data set will facilitate additional comparative analyses between changes in gene expression triggered by HBV and HCV infection; however, an initial comparison of microarray results between HBV- and HCV-infected PHHs demonstrate a much stronger stimulation of the innate immune response by HCV, which may support the notion that HBV is much more of a “stealth” virus. Interestingly, in our microarray experiments, we observed the upregulation of APOBEC3G, after HBV stimulation, which has recently been implicated in antiviral responses to HBV (data not shown) (37).

Lastly, we demonstrated that HBV stimulates innate immunity mainly through NF- κ B-dependent pathways, whereas HCV and DNA mimetics mainly activate both IRF3 and NF- κ B (2). A recent study has proposed that HBV triggers antiviral innate immunity through retinoic acid-inducible gene (RIG-I) activation from RNA produced from HBV’s DNA genome (30). In addition, other recent studies have demonstrated a role for the STING-TBK1-IRF3 in detection of HBV (35, 36). Our studies were unable to substantiate a role for the STING pathway in early HBV responses. We used HBV virions for our studies in PHHs and HepaRG cells, whereas the other studies used other hepatoma cell lines and transfected nucleic acids that stimulate stronger responses than that seen with HBV. Indeed, we validated the role of STING in responses to transfected DNA mimetics in hepatocytes demonstrating the functionality of our assays (Fig. 7A–D).

This study builds on these findings by implicating MDA5 as a receptor for RNA transcribed from the HBV DNA genome (5) and NF- κ B as the downstream transcription factor responsible for gene induction. The predominant activation of NF- κ B as opposed to IRF3 is compatible with the stronger inflammatory response. In addition, chronic NF- κ B activation may be important for the development of hepatocellular carcinoma in HBV-infected patients. Data

presented in Fig. 1D showing increased upregulation of CCL5, a gene we have found to be minimally stimulated by IFN (2), in the presence of both HBV and IFN indicates that genes stimulated by IFN, such as MDA5, can aid in the rapid innate immune response to HBV. However, a recent study has demonstrated that HBV has the ability to downregulate early antiviral responses (25). This ability to downregulate innate response would support the characterization of HBV as a “stealth” virus when compared with other viruses such as HCV.

In conclusion, our data demonstrate a significant rapid inflammatory response in several models of HBV stimulation. A proposed model of hepatocyte nucleic acid sensing is shown in Fig. 10. We believe the activation of this rapid innate response in hepatocytes drives the subsequent inflammatory responses that are responsible for recruitment of immune cells into the liver in HBV-infected patients. Further characterization of chemokine responses to HBV using appropriate models will add crucial insight into the pathogenesis of HBV infection and possibly provide innovative targets for therapeutic development against hepatitis B-triggered liver inflammation as well as novel strategies to target the degradation of cccDNA that can occur after treatment with type I IFN.

Disclosures

The authors have no financial conflicts of interest.

References

- Kawai, T., and S. Akira. 2009. The roles of TLRs, RLRs and NLRs in pathogen recognition. *Int. Immunol.* 21: 317–337.
- Thomas, E., V. D. Gonzalez, Q. Li, A. A. Modi, W. Chen, M. Nouredin, Y. Rotman, and T. J. Liang. 2012. HCV infection induces a unique hepatic innate immune response associated with robust production of type III interferons. *Gastroenterology* 142: 978–988.
- Rall, L. B., D. N. Standing, O. Laub, and W. J. Rutter. 1983. Transcription of hepatitis B virus by RNA polymerase II. *Mol. Cell. Biol.* 3: 1766–1773.
- Standing, D. N., L. B. Rall, O. Laub, and W. J. Rutter. 1983. Hepatitis B virus encodes an RNA polymerase III transcript. *Mol. Cell. Biol.* 3: 1774–1782.
- Jansen, L., N. A. Kootstra, K. A. van Dort, R. B. Takkenberg, H. W. Reesink, and H. L. Zaaijer. 2016. Hepatitis B virus pregenomic RNA is present in virions in plasma and is associated with a response to pegylated interferon alpha-2a and nucleos(t)ide analogues. *J. Infect. Dis.* 213: 224–232.
- Seeger, C. M. B., F. Zoulim. 2006. Hepadnaviruses. In *Field Virology*, 5th Ed. Vol. 2. D. M. Knipe and P. M. Howley, eds. Lippincott Williams & Wilkins, Philadelphia, p. 2185–2221.
- Wieland, S., R. Thimme, R. H. Purcell, and F. V. Chisari. 2004. Genomic analysis of the host response to hepatitis B virus infection. *Proc. Natl. Acad. Sci. USA* 101: 6669–6674.
- Wieland, S. F., and F. V. Chisari. 2005. Stealth and cunning: hepatitis B and hepatitis C viruses. *J. Virol.* 79: 9369–9380.
- Shlomai, A., R. E. Schwartz, V. Ramanan, A. Bhatta, Y. P. de Jong, S. N. Bhatia, and C. M. Rice. 2014. Modeling host interactions with hepatitis B virus using primary and induced pluripotent stem cell-derived hepatocellular systems. *Proc. Natl. Acad. Sci. USA* 111: 12193–12198.

10. Guidotti, L. G., R. Rochford, J. Chung, M. Shapiro, R. Purcell, and F. V. Chisari. 1999. Viral clearance without destruction of infected cells during acute HBV infection. *Science* 284: 825–829.
11. Stacey, A. R., P. J. Norris, L. Qin, E. A. Haygreen, E. Taylor, J. Heitman, M. Lebedeva, A. DeCamp, D. Li, D. Grove, et al. 2009. Induction of a striking systemic cytokine cascade prior to peak viremia in acute human immunodeficiency virus type 1 infection, in contrast to more modest and delayed responses in acute hepatitis B and C virus infections. *J. Virol.* 83: 3719–3733.
12. Dunn, C., D. Peppas, P. Khanna, G. Nebbia, M. Jones, N. Brendish, R. M. Lascar, D. Brown, R. J. Gilson, R. J. Tedder, et al. 2009. Temporal analysis of early immune responses in patients with acute hepatitis B virus infection. *Gastroenterology* 137: 1289–1300.
13. Tan, A. T., S. Koh, W. Goh, H. Y. Zhe, A. J. Gehring, S. G. Lim, and A. Bertoletti. 2010. A longitudinal analysis of innate and adaptive immune profile during hepatic flares in chronic hepatitis B. *J. Hepatol.* 52: 330–339.
14. Luangsang, S., M. Ait-Goughoulte, M. Michelet, O. Floriot, M. Bonnin, M. Gruffaz, M. Rivoire, S. Fletcher, H. Javanbakht, J. Lucifora, et al. 2015. Expression and functionality of Toll- and RIG-like receptors in HepaRG cells. *J. Hepatol.* 63: 1077–1085.
15. Giersch, K., L. Allweiss, T. Volz, M. Helbig, J. Bierwolf, A. W. Lohse, J. M. Pollok, J. Petersen, M. Dandri, and M. Lütgehetmann. 2015. Hepatitis Delta co-infection in humanized mice leads to pronounced induction of innate immune responses in comparison to HBV mono-infection. *J. Hepatol.* 63: 346–353.
16. Papatheodoridis, G., J. Goulis, S. Manolakopoulos, A. Margariti, X. Exarchos, G. Kokkonis, E. Hadziyiannis, C. Papaioannou, E. Manesis, D. Pectasides, and E. Akriviadis. 2014. Changes of HBsAg and interferon-inducible protein 10 serum levels in naive HBsAg-negative chronic hepatitis B patients under 4-year entecavir therapy. *J. Hepatol.* 60: 62–68.
17. Ishikawa, H., and G. N. Barber. 2008. STING is an endoplasmic reticulum adaptor that facilitates innate immune signalling. *Nature* 455: 674–678.
18. Ishii, K. J., C. Coban, H. Kato, K. Takahashi, Y. Torii, F. Takeshita, H. Ludwig, G. Sutter, K. Suzuki, H. Hemmi, et al. 2006. A Toll-like receptor-independent antiviral response induced by double-stranded B-form DNA. *Nat. Immunol.* 7: 40–48.
19. Chiu, Y. H., J. B. Macmillan, and Z. J. Chen. 2009. RNA polymerase III detects cytosolic DNA and induces type I interferons through the RIG-I pathway. *Cell* 138: 576–591.
20. Keskinen, P., M. Nyqvist, T. Sareneva, J. Pirhonen, K. Melén, and I. Julkunen. 1999. Impaired antiviral response in human hepatoma cells. *Virology* 263: 364–375.
21. Melén, K., P. Keskinen, A. Lehtonen, and I. Julkunen. 2000. Interferon-induced gene expression and signaling in human hepatoma cell lines. *J. Hepatol.* 33: 764–772.
22. Gripon, P., S. Rumin, S. Urban, J. Le Seyec, D. Glaise, I. Canne, C. Guyomard, J. Lucas, C. Trepo, and C. Guguen-Guillouzo. 2002. Infection of a human hepatoma cell line by hepatitis B virus. *Proc. Natl. Acad. Sci. USA* 99: 15655–15660.
23. Lucifora, J., D. Durantel, B. Testoni, O. Hantz, M. Levrero, and F. Zoulim. 2010. Control of hepatitis B virus replication by innate response of HepaRG cells. *Hepatology* 51: 63–72.
24. Sells, M. A., M. L. Chen, and G. Acs. 1987. Production of hepatitis B virus particles in Hep G2 cells transfected with cloned hepatitis B virus DNA. *Proc. Natl. Acad. Sci. USA* 84: 1005–1009.
25. Luangsang, S., M. Gruffaz, N. Isorce, B. Testoni, M. Michelet, S. Faure-Dupuy, S. Maadadi, M. Ait-Goughoulte, R. Parent, M. Rivoire, et al. 2015. Early inhibition of hepatocyte innate responses by hepatitis B virus. *J. Hepatol.* 63: 1314–1322.
26. Liu, Y., M. Hussain, S. Wong, S. K. Fung, H. J. Yim, and A. S. F. Lok. 2007. A genotype-independent real-time PCR assay for quantification of hepatitis B virus DNA. *J. Clin. Microbiol.* 45: 553–558.
27. Mason, A. L., L. Xu, L. Guo, M. Kuhns, and R. P. Perrillo. 1998. Molecular basis for persistent hepatitis B virus infection in the liver after clearance of serum hepatitis B surface antigen. *Hepatology* 27: 1736–1742.
28. Livak, K. J., and T. D. Schmittgen. 2001. Analysis of relative gene expression data using real-time quantitative PCR and the 2(-Delta Delta C(T)) Method. *Methods* 25: 402–408.
29. Ronsin, C., A. Pillet, C. Bali, and G. A. Denoyel. 2006. Evaluation of the COBAS AmpliPrep-total nucleic acid isolation-COBAS TaqMan hepatitis B virus (HBV) quantitative test and comparison to the VERSANT HBV DNA 3.0 assay. *J. Clin. Microbiol.* 44: 1390–1399.
30. Sato, S., K. Li, T. Kameyama, T. Hayashi, Y. Ishida, S. Murakami, T. Watanabe, S. Iijima, Y. Sakurai, K. Watashi, et al. 2015. The RNA sensor RIG-I dually functions as an innate sensor and direct antiviral factor for hepatitis B virus. *Immunity* 42: 123–132.
31. Paludan, S. R., and A. G. Bowie. 2013. Immune sensing of DNA. *Immunity* 38: 870–880.
32. Zhang, X., H. Shi, J. Wu, X. Zhang, L. Sun, C. Chen, and Z. J. Chen. 2013. Cyclic GMP-AMP containing mixed phosphodiester linkages is an endogenous high-affinity ligand for STING. *Mol. Cell* 51: 226–235.
33. Dempsey, A., and A. G. Bowie. 2015. Innate immune recognition of DNA: a recent history. *Virology* 479–480: 146–152.
34. Bürckstümmer, T., C. Baumann, S. Blüml, E. Dixit, G. Dürnberger, H. Jahn, M. Planyavsky, M. Bilban, J. Colinge, K. L. Bennett, and G. Superti-Furga. 2009. An orthogonal proteomic-genomic screen identifies AIM2 as a cytoplasmic DNA sensor for the inflammasome. *Nat. Immunol.* 10: 266–272.
35. Cui, X., D. N. Clark, K. Liu, X. D. Xu, J. T. Guo, and J. Hu. 2015. Viral DNA-dependent induction of innate immune response to hepatitis B virus in immortalized mouse hepatocytes. *J. Virol.* 90: 486–496.
36. Dansako, H., Y. Ueda, N. Okumura, S. Satoh, M. Sugiyama, M. Mizokami, M. Ikeda, and N. Kato. 2016. The cyclic GMP-AMP synthetase-STING signaling pathway is required for both the innate immune response against HBV and the suppression of HBV assembly. *FEBS J.* 283: 144–156.
37. Lucifora, J., Y. Xia, F. Reisinger, K. Zhang, D. Stadler, X. Cheng, M. F. Sprinzl, H. Koppensteiner, Z. Makowska, T. Volz, et al. 2014. Specific and nonhepatotoxic degradation of nuclear hepatitis B virus cccDNA. *Science* 343: 1221–1228.